References

[1] Catherall, D., Stewartson, K., and Williams, P. G., "Viscous Flow Past a Flat Plate with Uniform Injection," *Proceedings of the Royal Society of London, Ser. A*, Vol. 284, March 1965, pp. 370–396.

[2] Lees, L. and Chapkis, R., "Surface Mass Injection at Supersonic and Hypersonic Speeds as a Problem in Turbulent Mixing," *AIAA Journal*, Vol. 7, No. 4, April 1969, pp. 671–680; also AIAA Paper 68-130, New York, Jan. 1968.

[3] Thomas, P. E., "Compressible Flow Over a Finite Flat Plate with Massive Blowing," Rept. 61-78-68-8, March 1968, Lockheed Research Lab., Palo Alto, Calif.

[4] Kubota, T. and Fernandez, F. L., "Boundary-Layer Flows with Large Injection and Heat Transfer," *AIAA Journal*, Vol. 6, No. 1, Jan. 1968, pp. 22–58.

[5] Reeves, B. L. and Lees, L., "Supersonic Separated and Reattaching Flows: I. General Theory and Application to Adiabatic Boundary-Layer/Shock-Wave Interactions" *AIAA Journal*, Vol. 2, No. 11, Nov. 1964, pp. 1907–1920.

[6] Fernandez, F. L. and Zukoski, E., "Experiments in Supersonic Turbulent Flow with Large Distributed Surface Injection," *AIAA Journal*, Vol. 7, No. 9, Sept. 1969, pp. 1759–1767; also AIAA Paper 68-129, New York, Jan. 1968.

[7] Stewartson, K., "Correlated Incompressible and Compressible Boundary Layers," *Proceedings of the Royal Society*, A200, Dec. 22, 1949, London, pp. 84–100.

[8] Coles, D. F., "The Turbulent Boundary Layer in a Compressible Fluid," *The Physics of Fluids*, Vol. 9, 1964, p. 1403.

[9] Klineberg, J. M., "Theory of Laminar Viscous-Inviscid Interaction in Supersonic Flow," Ph.D. thesis, June 1968, California Institute of Technology, Pasadena, Calif.

[10] Ko, D. R. S. and Kubota, T., "Supersonic Laminar Boundary Layer along a Two-Dimensional Adiabatic Curved Ramp," *AIAA Journal*, Vol. 7, No. 2, Feb. 1969, pp. 278–304; also AIAA Paper 68-109, New York, Jan. 1968.

[11] Victoria, K. J., "Hypersonic Laminar Boundary Layer Near a Sharp Expansion Corner," Ph.D. thesis, 1969, California Institute of Technology, Pasadena, Calif.

[12] Bradshaw, P., "The Turbulence Structure of Equilibrium Boundary Layers," *Journal of Fluid Mechanics*, Vol. 29, 1967, Pt. A, pp. 625–645.

[13] Liepmann, H. W. and Laufer, J., "Investigation of Free Turbulent Mixing," TN 1257, Aug. 1947, NACA.

JULY 1970 AIAA JOURNAL VOL. 8, NO. 7

Nonequilibrium, Ionized, Hypersonic Flow over a Blunt Body at Low Reynolds Number

SANG-WOOK KANG*

Cornell Aeronautical Laboratory, Inc., Buffalo, N. Y.

Ionized nonequilibrium flow in the forebody region (downstream as well as the stagnation) of a catalytic blunt body is theoretically analyzed in the incipient merged-layer regime using the thin shock-layer assumption. The species conservation equations for seven species and six chemical reactions are considered; they are decoupled from the momentum and the energy equations. Nonsimilar solutions are obtained by application of an integral method approach for various degrees of rarefaction. The results show sizable effects of wall cooling and species diffusion on the dissociation and the ionization levels, demonstrating in the process that the inviscid flow analysis overpredicts the electron-density level by as much as two orders of magnitude in the stagnation region and by three orders of magnitude in the downstream region of a catalytic blunt body. In addition, the results suggest that the binary scaling principle may be applied to the case of an ionized merged-layer flow over a blunt body at high altitudes.

Nomenclature

a = body nose radius, cm
C_i = mass fraction of ith species, gm_i/gm of mixture
C_{pi} = specific heat at constant pressure of ith species, cal/g_i − °K
D_i = binary diffusion coefficient of ith species, cm²/sec
E_i = surface-concentration gradient parameter of ith species, $\equiv (\partial C_i/\partial F)_b$
F = transformed normal coordinate, Eq. (12)
f = dimensionless stream function
G = parameter for shock standoff distance, Eq. (12)
H = total enthalpy, $h + (u^2 + v^2)/2$, cal/gm or atm-cm³/g
h_i = static enthalpy of ith species, $h_i^0 + \int_0^T C_{pi}dT$, cal/$g_i$
h_i^0 = heat of formation of ith species, cal/g_i
h = static enthalpy, $\Sigma_i C_i h_i$, cal/g of mixture
j = unity for axisymmetric flow and zero for planar flow
k_{fj} = forward reaction rate for the jth reaction, cm³/$mole_i$-sec
k_{bj} = backward reaction rate for the jth reaction, cm³/$mole_i$-sec, or cm⁶/$mole_i^2$-sec
K^2 = rarefaction parameter, $\epsilon(\rho_\infty U_\infty a/\mu)$
Le_i = Lewis number of ith species, Pr/Sc_i
m_i = molecular weight of ith species, g_i/g $mole_i$
n_i = mole fraction of ith species, C_i/m_i, $mole_i$/g of mixture
N_0 = Avogadro's number, 6.025×10^{23} particles/mole
p = pressure, atm
Pr = Prandtl number
$\mathfrak{R}$ = universal gas constant, 82.06 atm-cm³/gm mole − °K
r = distance from the axis to the body surface, cm
Sc_i = Schmidt number of ith species
T = temperature, °K
U = dimensionless streamwise velocity, $u/(U_\infty z)$
U_∞ = freestream velocity, cm/sec
u,v = velocities in physical coordinates (Fig. 1)
x,y = physical coordinates (Fig. 1)
z = r/a
β = shock angle
γ = specific heat ratio
Δ = shock standoff distance, cm
ϵ = $(\gamma - 1)/(2\gamma)$
Θ = total-enthalpy ratio, $(H - H_b)/(H_\infty - H_b)$

Received June 2, 1969; revision received December 11, 1969. This work was supported by NASA Goddard Space Flight Center, under Contract NAS 5-9978. The author wishes to acknowledge the useful discussions with M. G. Dunn and J. A. Lordi, and the assistance of J. R. Moselle in obtaining numerical solutions.

* Principal Engineer, Aerodynamic Research Department. Member AIAA.

μ = viscosity, gm/cm-sec
ξ = dimensionless streamwise distance, x/a
ρ = density, gm/cm^3
σ_e = electron number density, particles/cm^3
τ = temperature parameter, Eq. (19)
τ_j^0 = energy of formation of jth species, $h_j^0 m_j/\Re$, °K
ψ = stream function
Ω_i = species-concentration integral of ith species, e.g., Eq. (21)
w_i = production rate of ith species, jm$_i$/cm^3-sec

Subscripts

b = body surface
i = ith species
∞ = freestream condition

I. Introduction

ANALYSIS of the flow about a blunt body at hypersonic speeds has received much attention in recent years because of its relevance to the design of the heat-protection system, to understanding the communications blackout problem, and to predicting aerodynamic forces. At the higher altitudes the blunt-body flow is complicated by the combined presence of chemical nonequilibrium (including ionization) phenomena and rarefaction effects that can result in a fully viscous shock layer. Although these phenomena have been analyzed separately, they have not been treated simultaneously for the entire flowfield. It is the purpose of the present analysis to investigate theoretically the ionized nonequilibrium flow of a multispecies air in the fully viscous merged-layer regime. An integral method approach is applied to the forebody region (downstream as well as stagnation) of a blunt body under the assumption that the species conservation equations are uncoupled from the fluid dynamic conservation equations.

A brief review of previous analyses as well as a short outline of the present approach will be given in this section, while the method of solution and the discussion of the results obtained from the present analysis will be included in Secs. II and III, respectively.

In analyzing the chemical nonequilibrium nature of the flow, studies were based on the inviscid flow model[1,2] in gaining a first-order insight into actual problems. However, this approximation is applicable only at lower altitudes where the viscous effects are confined to a very thin layer near the body surface. Since an inviscid model does not allow for any energy transfer to the body, the analysis tends to overpredict the electron density for a given flight condition, resulting in an upper-bound estimate of the ionization levels. Analysis of the nonequilibrium flow in the thin boundary layer has been performed, for example, for slender bodies.[3] The electron-density levels are generally lower than the maximum level obtained from an inviscid flow model. Again the boundary-layer approximation is valid at lower altitudes only and is not applicable at high altitudes, where the layer surrounding the body is a fully viscous shock layer.[4]

In regard to the effects of rarefaction on the chemically reacting flow, studies[5,6] have been made for a binary gas in the stagnation region of a blunt body. Because a binary gas is considered, only one equation for the atom species needs to be solved. The analysis is further simplified in the stagnation region in that ordinary differential equations result there, that is, the independent variable of importance is the coordinate normal to the body surface. The results thus obtained show the influence of rarefaction on the flow to be appreciable, especially on the concentration level of the atoms. In particular, the atom concentration level decreases with increasing rarefaction. Additionally, Cheng's work[6] demonstrated the large influences of diffusion and wall temperature on the atom concentration levels in the viscous shock layer. Subsequently, results were obtained for ionized air in the stagnation region at high altitudes,[7,8] and comparison of the results with an inviscid analysis indicates that the rarefaction reduces the electron concentration level by as much as a factor of 100 in the stagnation region. One major result obtained by these analyses is that the binary scaling principle may be applied for an ionized flow in the stagnation region of a blunt body at high altitudes because of the dominant two-body collision processes. This is an important result, since for the same freestream velocity it enables prediction of results at different altitudes and different body-nose radii in terms of the results obtained at a given altitude and nose radii, as long as $\rho_\infty a$ = constant, where ρ_∞ denotes the ambient density and a the body-nose radius. It is an additional purpose of the present analysis (which considers the entire forebody region of a blunt body) to determine whether the binary scaling principle may also be reasonably applied in the downstream region at high altitudes.

In the present formulation, an axisymmetric (or two-dimensional) ionized flow over a blunt body with a catalytic surface is considered. The flow will be in the incipient merged-layer regime in which the Navier-Stokes equations may be used,[4,6,9] and the normal momentum and the streamwise momentum equations are simplified by assuming a very thin shock layer compared with the body radius. In addition, the body is taken to be spherical so that the radius of curvature a is a constant. The streamwise velocity component as well as the temperature jump effects at the body surface are assumed to be zero, implying a no-slip condition which is reasonable for a cold wall[6] case. The nonequilibrium ionized nature of the flow is described by the species conservation equations for a seven-species air undergoing six reactions.

II. Formulation of Analysis

A. Assumptions

In order to simplify the analysis while retaining the essential features of the physical flow, the following assumptions are introduced: 1) a thin shock layer, 2) two-layer model of Cheng,[6] 3) constant Prandtl and Schmidt numbers, 4) binary diffusion due to concentration gradient only, 5) negligible changes in the flow properties due to the chemical reactions in the flowfield, 6) negligible nonequilibrium effects due to electronic and vibrational relaxation, and 7) ambipolar diffusion for the electrons and ions. These assumptions have been made in part or wholly in the previous analyses and the rationale for these assumptions may be found in Refs. 4, 6, 7, 9, and 10. However, justifications for some of these assumptions will be reiterated in appropriate sections in the present analysis.

B. Basic Equations

With the preceding assumptions the governing equations for the viscous, ionized shock layer in the incipient merged-layer regime become[6,9,11] (see Fig. 1 for a description of the flowfield):

$$\partial/\partial x(\rho u r^i) + \partial/\partial y(\rho v r^i) = 0 \tag{1}$$

$$\rho u \partial u/\partial x + \rho v \partial u/\partial y = (\partial/\partial y)(\mu \partial u/\partial y) \tag{2}$$

$$\rho u^2/a = \partial p/\partial y \tag{3}$$

$$\rho u \frac{\partial H}{\partial x} + \rho v \frac{\partial H}{\partial y} = \frac{\partial}{\partial y}\left\{\frac{\mu}{Pr} \cdot \frac{\partial}{\partial y}\left[H + (Pr - 1)\frac{u^2}{2}\right]\right\} + \frac{\partial}{\partial y}\left\{\frac{\mu}{Pr}(Le - 1)\sum_i h_i \frac{\partial C_i}{\partial y}\right\} \tag{4}$$

$$\rho u \frac{\partial C_i}{\partial x} + \rho v \frac{\partial C_i}{\partial y} = \frac{\partial}{\partial y}\left(\rho D_i \frac{\partial C_i}{\partial y}\right) + w_i \tag{5}$$

$$p = \rho \Re T \sum_i C_i/m_i \tag{6}$$

These equations express the conservation of mass, mo-

mentum, energy, and chemical species, respectively, along with an equation of state. The seven species considered are: O_2, N_2, O, N, NO, NO^+, e^-. With the two-layer model of Cheng,[6] these equations are applied to the viscous shock layer allowing for the diffusion of the species into the shock-transition zone by using the modified Rankine-Hugoniot conditions. Analysis of the entire flowfield performed in Ref. 10 reinforces the applicability of the two-layer model, and only the viscous shock layer will be considered in the present analysis. The boundary conditions for a fully catalytic solid wall are[6]

at $y = 0$,

$$u = 0 = v,\ H = H_b(x),\ p = p_b(x)$$
$$C_i = 0,\ (\mathrm{N,O,NO,NO^+,e^-}) \qquad (7)$$
$$C_i = C_i(\infty),\ (\mathrm{O_2,N_2})$$

at $y = \Delta(x)$,

$$u = U_\infty \cos\beta - (\mu/\rho_\infty u_\infty \sin\beta)\cdot\partial u/\partial y$$
$$p \cong \rho_\infty U_\infty^2 \sin^2\beta$$
$$H = H_\infty - (\mu/Pr\rho_\infty U_\infty \sin\beta)\cdot(\partial/\partial y) \times \{H + [(Pr - 1)/2]u^2\} \qquad (8)$$
$$C_i = -(\mu/Sc_i\rho_\infty U_\infty \sin\beta)\cdot\partial C_i/\partial y$$

The molecular concentrations can be expressed in terms of the other species by locally conserving the elemental composition, yielding

$$C_{O_2}(y) = C_{O_2}(\infty) - C_O(y) - (m_O/m_{NO})C_{NO}(y)$$
$$C_{N_2}(y) = C_{N_2}(\infty) - C_N(y) - (m_N/m_{NO})C_{NO}(y), \qquad (9)$$

where $C_{N_2}(\infty) = 0.767$ and $C_{O_2}(\infty) = 0.233$.

The total enthalpy H is expressed in terms of T and C_i such that

$$H = \frac{u^2 + v^2}{2} + \sum_i C_i\left(h_i^0 + \int_0^T C_{p_i}dT\right) \qquad (10)$$

C. Chemical-Reaction Model

The chemical reactions considered simultaneously for air dissociation and ionization are as follows:[12,13]

$$O_2 + M + 5.12^{ev} \underset{k_b}{\overset{k_f}{\rightleftarrows}} 2O + M$$
$$N_2 + M + 9.76^{ev} \rightleftarrows 2N + M$$
$$NO + M + 6.49^{ev} \rightleftarrows N + O + M \qquad (11)$$
$$NO + O + 1.37^{ev} \rightleftarrows O_2 + N$$
$$N_2 + O + 3.27^{ev} \rightleftarrows NO + N$$
$$N + O + 2.76^{ev} \rightleftarrows NO^+ + e^-$$

For the forward and the backward reaction rates, k_f and k_b, and the various species production rates (w_i), those suggested by Wray[12] have been used except for the last reaction, for which the rate obtained by Dunn and Lordi[14] was used. These rates are shown in Table 1. A discussion of the chemical reaction processes is given in Appendix A.

D. Method of Analysis

In solving the Eqs. (1–6) with the boundary conditions and the chemical reactions described in the previous section, the following transformation is made:[11]

$$\xi \equiv \frac{x}{a},\ F \equiv \frac{1}{G}\int_0^y \frac{\rho}{\rho_\infty}\frac{dy}{a},\ G \equiv \int_0^{\Delta(x)} \frac{\rho}{\rho_\infty}\frac{dy}{a} \qquad (12)$$

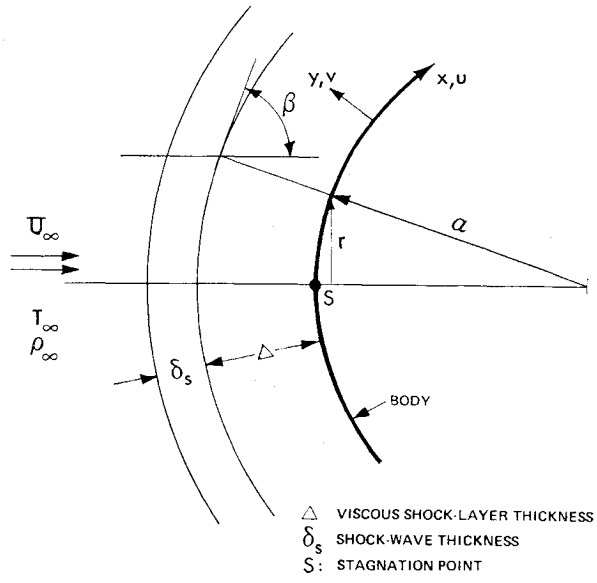

Fig. 1 Co-ordinate system.

In addition a stream function ψ is introduced such that $\partial\psi/\partial x = -(1 + j)(\pi r)^j\rho v$ and $\partial\psi/\partial y = (1 + j)(\pi r)^j\rho u$, which satisfies the continuity equation (1). A dimensionless stream function $f(\xi,F)$ is now obtained by putting $\psi = (1 + j)\rho_\infty U_\infty r(\pi r)^j f$, which yields the relationship $\partial f/\partial F = UG$, where $U \equiv u/(U_\infty z)$. Here $z = r/a$ and is taken to be equal to $\cos\beta$, consistent with the thin shock-layer approximation.[6]

Transformation of Eqs. (2–5) yields, after some rearrangement

$$\frac{\partial^3 f}{\partial F^3} = K^2G\left[\frac{dz}{d\xi}\cdot\left(\frac{\partial f}{\partial F}\right)^2 - (1 + j)\frac{dz}{d\xi}\cdot f\cdot\frac{\partial^2 f}{\partial F^2} + zG\left(\frac{\partial f}{\partial F}\right)\cdot\frac{\partial}{\partial\xi}\left(\frac{1}{G}\cdot\frac{\partial f}{\partial F}\right) - z\frac{\partial f}{\partial\xi}\cdot\frac{\partial^2 f}{\partial F^2}\right] \qquad (13)$$

$$\partial p/\partial F = (\rho_\infty U_\infty^2 z^2/G)(\partial f/\partial F)^2 \qquad (14)$$

$$z(1 - t_b)\left(\frac{\partial f}{\partial F}\frac{\partial\theta}{\partial\xi} - \frac{\partial f}{\partial\xi}\frac{\partial\theta}{\partial F}\right) + z\frac{dt_b}{d\xi}\cdot\frac{\partial f}{\partial F}\cdot(1 - \Theta) - (1 + j)(1 - t_b)\frac{dz}{d\xi}f\frac{\partial\theta}{\partial F} = \frac{1 - t_b}{PrK^2G}\frac{\partial^2\theta}{\partial F^2} + \frac{Pr - 1}{Pr}\cdot\frac{2z^2}{K^2G^3}\cdot\frac{\partial}{\partial F}\left(\frac{\partial f}{\partial F}\cdot\frac{\partial^2 f}{\partial F^2}\right) \qquad (15)$$

and

$$z\left(\frac{\partial f}{\partial F}\frac{\partial C_i}{\partial\xi} - \frac{\partial f}{\partial\xi}\frac{\partial C_i}{\partial F}\right) - (1 + j)\frac{dz}{d\xi}f\frac{\partial C_i}{\partial F} = \frac{1}{Sc_iK^2G}\cdot\frac{\partial^2 C_i}{\partial F_2} + \frac{aG}{U_\infty}\cdot\frac{w_i}{\rho} \qquad (16)$$

where $Sc_i = \mu/(\rho D_i)$, $t_b = H_b/H_\infty$, $\Theta = (H - H_b)/(H_\infty - H_b)$ and K^2 is the rarefaction parameter due to Cheng.[6] The term G corresponds to the shock layer thickness in the transformed coordinate system.

The Eqs. (13–16) should be considered simultaneously with appropriate boundary conditions. However, the previous results obtained, especially those by Chung, Holt, and Liu,[10] indicate that for low Reynolds numbers the flowfield properties such as the pressure, velocity, and enthalpy change very little despite the presence of chemical reactions in the flow. Thus, in the present study, the fluid dynamics equations, Eqs. (13–15), are decoupled from the species conservation equations in an effort to simplify the analysis without great loss in accuracy. This assumption has also been made by Lee

Table 1 Reaction rates for chemical processes

Reaction	Catalyst M	Equilibrium constant ($K_c = k_f/k_b$)	Rate constant expression
$O_2 + M \underset{k_{b1}}{\overset{k_{f1}}{\rightleftarrows}} 2O + M$ (5.1 ev)	N,NO:	$k_{f_1} = (3.6)(10^{18})T^{-1}\exp(-59{,}500/T)$	$K_c = (1.2)(10^3)T^{-0.5}\exp(-59{,}500/T)$ $T(°K)$, K_c (moles/cm³)
	N_2:	$k_f = 2k_{f_1}$	
	O_2:	$k_f = 9k_{f_1}$	
	O:	$k_f = 25\,k_{f_1}$	
$N_2 + M \underset{}{\overset{k_{f2}}{\rightleftarrows}} 2N + M$ (9.8 ev)	O,O_2,NO:	$k_{f_2} = (1.9)(10^{17})T^{-0.5}\exp(-113{,}000/T)$	$K_c = 18\exp(-113{,}000/T)$ K_c (moles/cm³)
	N_2:	$k_f = 2.47\,k_{f_2}$	
	N:	$k_f = (2.15)(10^5)T^{-1}k_{f_2}$	
$NO + M \rightleftarrows N + O + M$ (6.5 ev)	O_2,N_2:	$k_{f_3} = (3.9)(10^{20})T^{-1.5}\exp(-75{,}500/T)$	$K_c = 4\exp(-75{,}500/T)$ K_c (moles/cm³)
	NO,O,N:	$k_f = 20\,k_{f_3}$	
$NO + O \rightleftarrows O_2 + N$ (1.4 ev)		$k_{f_4} = (3.2)(10^9)T\exp(-19{,}700/T)$	$K_c = 0.24\exp(-16{,}120/T)$
$N_2 + O \rightleftarrows NO + N$ (3.3 ev)		$k_{f_5} = (7)(10^{12})\exp(-38{,}000/T)$	$K_c = 4.5\exp(-38{,}000/T)$
$N + O \rightleftarrows NO^+ + e^-$ (2.8 ev)		$k_{f_6} = (1.94)(10^{12})\exp(-31{,}900/T)$	$K_c = (3.6)(10^{-10})T^{1.5}\exp(-31{,}900/T)$

and Zierten[7] in their analysis of the stagnation region and meaningful results were obtained for the species distributions. Thus, these flow properties are considered to be known quantities in solving for the species concentrations. In the present study, the flow conditions in the downstream region of a blunt body are required, and the flow properties previously obtained by Kang[11] will be used; in particular, the distributions of the streamwise velocity (U), the pressure (p), and the total enthalpy (Θ) obtained in the stagnation as well as in the downstream regions in Ref. 11 will be used as inputs to the species-conservation equations. The static temperature (T), on the other hand, is sensitive to the chemical reactions present in the viscous shock layer, and must be considered as a part of the present problem. It may be expressed as, putting $H_\infty \sim U_\infty^2/2$

$$T(\xi,F) = H_\infty \tau(\xi,F)/Cp(\xi,F) \tag{17}$$

where

$$C_p \equiv \sum_i C_i C_{pi},\ (i = N,O,NO,O_2,N_2,NO^+,e^-) \tag{18}$$

$$\tau \equiv t_b + (1 - t_b)\Theta - z^2U^2 - (\Re/H_\infty)\sum_j C_i\tau_i^0/m_i,\ (j = N,O,NO,NO^+,e^-) \tag{19}$$

and

$$\tau_j^0 \equiv h_j^0 m_j/\Re$$

The density term also changes with the chemical reactions present in the flowfield and may be expressed from the equation of state,

$$\rho = p/(\Re T\sum_i C_i/m_i)$$

Thus the problem now is to simultaneously solve the species-conservation Eq. (16) for O, N, NO, and NO^+. The concentration levels for the molecules O_2 and N_2 are then obtained from Eq. (9) and the electron-density level may be obtained from the relationship $n_{e^-} = n_{NO^+}$, or $C_{e^-} = (m_{e^-})(C_{NO^+}/m_{NO^+})$, which yields in particles per cm³,

$$\sigma_e = N_0\rho C_{e^-}/m_{e^-} \tag{20}$$

where N_0 is the Avogadro's number.

In analyzing the present problem, the Kármán-Pohlhausen integral method approach has been used in order to obtain solutions because of the advantages of the method over the more complex exact method (which requires in most cases solution of the "two-point" boundary-value problem, or the use of an expansion scheme). These advantages are the ease of application and the relatively small computation time. In addition, the integral method has been shown to be applicable to the case of nonequilibrium flow,[15] and to the case of merged-layer flow.[11,16] Thus, integrating the species-conservation Eqs. (16) from $F = 0$ to $F = 1$, we obtain, after a series of rearrangements for O, N, NO and NO^+,

$$\frac{d\Omega_O}{d\xi} = z^j\left(\frac{dz}{d\xi} + \frac{E_O}{S_{cO}K^2G} - \frac{aG}{U_\infty}\int_0^1 \frac{w_O}{\rho}\,dF\right) \tag{21}$$

$$\frac{d\Omega_N}{d\xi} = z^j\left(\frac{dz}{d\xi} + \frac{E_N}{S_{cN}K^2G} - \frac{aG}{U_\infty}\int_0^1 \frac{w_N}{\rho}\,dF\right) \tag{22}$$

$$\frac{d\Omega_{NO}}{d\xi} = z^j\left(\frac{dz}{d\xi} + \frac{E_{NO}}{S_{cNO}K^2G} - \frac{aG}{U_\infty}\int_0^1 \frac{w_{NO}}{\rho}\,dF\right) \tag{23}$$

and

$$\frac{d\Omega_{NO^+}}{d\xi} = z^j\left(\frac{dz}{d\xi} + \frac{E_{NO^+}}{S_{cNO^+}K^2G} - \frac{aG}{U_\infty}\int_0^1 \frac{w_{NO^+}}{\rho}\,dF\right) \tag{24}$$

where

$$\Omega_i \equiv Gz^{1+j}\int_0^1 U(1 - C_i)dF \quad \text{and} \quad E_i \equiv \left(\frac{\partial C_i}{\partial F}\right)_b$$

By substitution of the various species profiles C_i (see Appendix B for details of derivation) and of the streamwise velocity profile (U) previously obtained[11] in the definition of Ω_i, we obtain expressions for these quantities in terms of four unknown parameters E_O, E_N, E_{NO}, and E_{NO^+}. Other terms such as K^2, t_b, G, etc., are specified as known quantities. Since the species production term w_i contains not only the temperature term but other species terms as well (C_O,C_N,C_{NO}, etc.), (see Appendix A), it is necessary to solve Eqs. (21–24) simultaneously. Thus the problem is to determine from Eqs. (21–24) the four unknown parameters E_i (i = O,N,NO and NO^+) as functions of the streamwise distance ξ. The term E_i denotes the local concentration-gradient parameter in the transformed coordinate system. Details of the determination of these quantities for various values of the rarefaction parameter K^2 and the discussion of the results obtained will be presented in the following section.

III. Solutions and Discussion of Results

A. Integration Procedure

For given values of the rarefaction parameter, the surface enthalpy ratio and the flow properties such as velocity, pressure, and enthalpy, the Eqs. (21–24) were numerically integrated along the streamwise distance to yield solutions in terms of the unknown parameters E_N, E_O, E_{NO}, and E_{NO^+}. These parameters are then used to describe other flow quantities of interest in the viscous hypersonic ionized flow, such

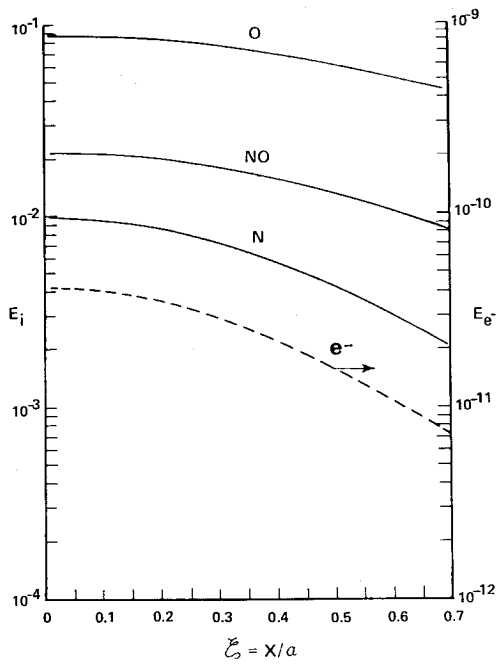

Fig. 2 Distributions of the species-gradient parameter along a blunt body ($K^2 = 5$).

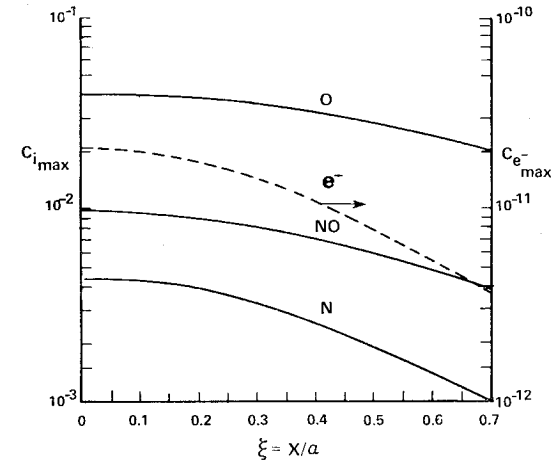

Fig. 3 Maximum species concentrations over a blunt body ($K^2 = 5$).

as the various species profiles, the species distributions, and the maximum electron-density values in the stagnation region as well as in the downstream region.

In obtaining solutions, conditions were first calculated in the stagnation region by specializing Eqs. (21–24) to that region. These solutions were then used as initial conditions in solving Eqs. (21–24) in the downstream direction. The numerical-integration scheme adopted was the Adams-Molton predictor-corrector method and the computation time for integration along ξ up to $\xi \cong 0.9$ for a single typical case was about 1.5 min on the IBM 360 computer. Solutions were obtained for K^2 between 0.1 and 10, which is the approximate range for the incipient merged-layer regime. Other flow properties taken were $t_b = 0.05$ (cold wall), $U_\infty = 23{,}000$ fps, $Pr = 0.75$, with the Schmidt number for the neutral species taken to be 0.75 and the Schmidt number for the ions and electrons taken to be 0.375. For a body nose radius a of 1 ft, $K^2 = 10$ corresponds to an altitude of about 290,000 ft and $K^2 = 0.1$ to a 390,000 ft altitude.[6] All the results obtained display similar behavior, and only typical results are presented here. Detailed results are given in Ref. 17.

B. Results

Figure 2 shows the distributions of the parameter E for O, N, NO and e^- along the streamwise distance from the stagnation region of a blunt body for the case $K^2 = 5$. The term E denotes the surface-gradient of the chemical species and thus represents a measure of the flux of the species impinging on the body surface. In conjunction with Fig. 3, which shows the distributions of the maximum species concentrations along the streamwise distance, these results demonstrate that the levels of dissociation are greatest in the stagnation region and gradually decrease in the downstream region. Physically, this result is due to the fact that the temperature is generally higher along the stagnation line than in the downstream region and causes greater dissociation, as shown in Fig. 4. As was pointed out in the analysis of the stagnation region in Ref. 7, the levels of the species concentrations are lower than the inviscid case by about an order of magnitude. This is primarily due to the diffusion of the species to the catalytic wall and to the shock-transition zone and also due to the wall cooling extending all the way to the shock wave, thus reducing the temperature in the viscous shock layer. The present results confirm this trend in the stagnation region and further indicate that these same influences exist in the downstream region as well. The temperature profiles in Fig. 4 show also that the temperature gradients at the body surface decrease in the streamwise direction, indicating the lowering of the heat-transfer rate to the body, consistent with the previous results obtained for the thin boundary-layer flow[18,19] and for the merged-layer flow along a blunt body.[11]

The variations in the maximum values of the dissociation products (O,N,NO,NO^+ and e^-) with the rarefaction are shown for the stagnation region in Fig. 5. They demonstrate sizable reductions with increasing rarefaction, with the electron level displaying the greatest sensitivity to rarefaction. This is due to the lowered temperatures in the merged layer and the resultant low concentration levels for the oxygen and the nitrogen atoms, as well as to the lowered ionization rate. For K^2 below 2.0, the dissociation levels are very small and thus the flow may be considered to be frozen. Based on the results shown in Fig. 5, the maximum electron density levels are obtained for various values of the rarefaction parameter by use of Eq. (20). They are shown in Fig. 6 for the case of an Apollo body whose nose radius is 474 cm. For this case $K^2 = 10$ corresponds to an altitude of about 340,000 ft, $K^2 = 5$ to 360,000 ft, and $K^2 = 1$ to about 390,000 ft. It may be seen from the figure that for $K^2 = 10$ the maximum electron density level in the stagnation region is

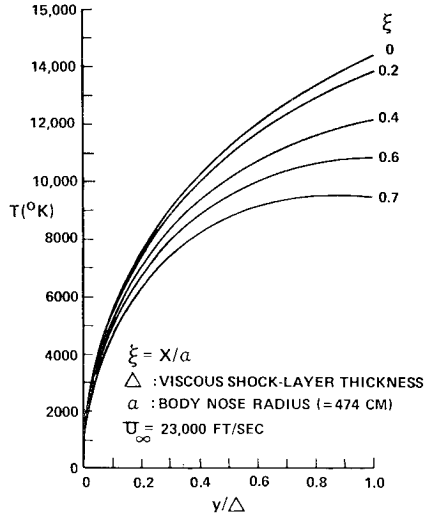

Fig. 4 Distributions of temperature profiles along a blunt body ($K^2 = 5$).

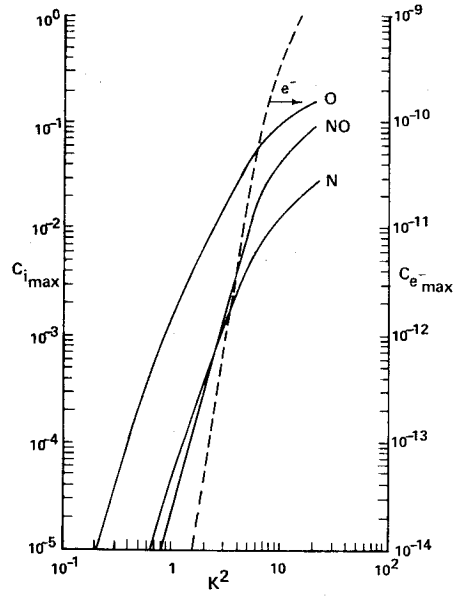

Fig. 5 Maximum species concentrations for various rarefaction in the stagnation region.

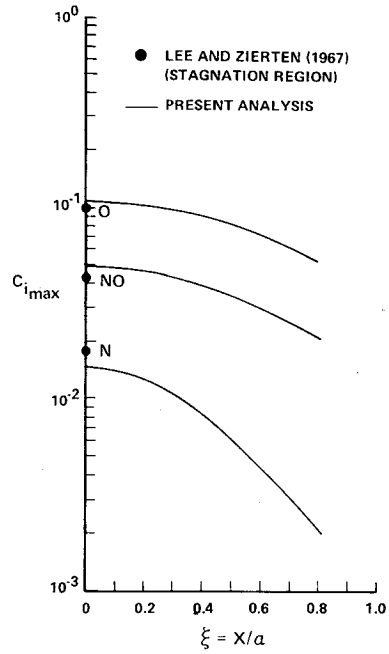

Fig. 7 Distributions of the maximum species concentrations along the body, and comparison with exact (numerical) solutions.

$2(10^9)$ particles/cm^3, decreasing in the downstream direction to $3(10^8)$ particles/cm^3 at $\xi \sim 0.7$, a reduction by about an order of magnitude. At higher altitudes, that is, as K^2 decreases, the electron-density levels are sharply reduced, so that for $K^2 = 1$ they are $4.7(10^2)$ particles/cm^3 in the stagnation region and only 9 particles/cm^3 at $\xi \sim 0.7$, indicating that practically no ionization exists at this altitude. Coupled with the negligible levels of the dissociation products (O,N, NO) at this condition, these results demonstrate the sizable influence of rarefaction on the chemistry of the flow in the viscous shock layer.

In assessing the accuracy of the present results, comparison should be made with more exact analyses. No exact analysis, however, appears to exist which treats the present problem of a merged-layer ionization in the entire forebody region of a blunt body. However, analysis for the special case of the ionization in the stagnation region has been made by Lee and Zierten[7] and comparisons will be made with their results in the stagnation region. Figures 7 and 8 show the comparisons for the maximum levels of the neutral species and of the electron number density. Lee and Zierten[7] considered the case of $a = 0.675$ in. and $U_\infty = 23{,}000$ fps at 227,000 ft altitude, which corresponds to the rarefaction value of $K^2 \sim 12$. Their results are compared with the present results in Figs. 7 and 8 in terms of the maximum levels of the dissociation products (O,N,NO and e^-). Good agreement is noted between the two results, especially for the maximum electron density level, which is at approximately $3(10^{11})$ particles/cm^3 in the stagnation region. Similarly favorable comparison has been made for the 215,000 ft altitude case. As pointed out in Ref. 7, the inviscid results are greater than the present values by a factor of 100 in the stagnation region. The calculations performed for this case based on an inviscid flow model[1] indicate that the overpredication of the ionization levels are even greater in the downstream region. For example, the inviscid results showed that the maximum electron-density level is reduced at $\xi \sim 0.7$ by a factor of about 2 from the stagnation value, while the present results for the merged-layer case (Fig. 8) show a reduction of an

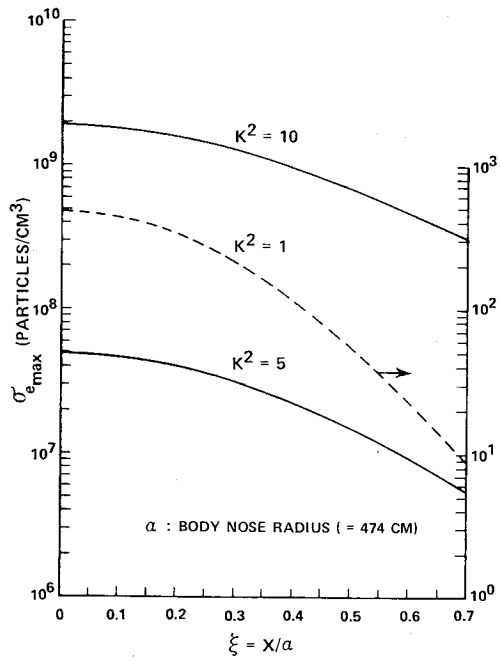

Fig. 6 Maximum electron-density levels over a blunt body.

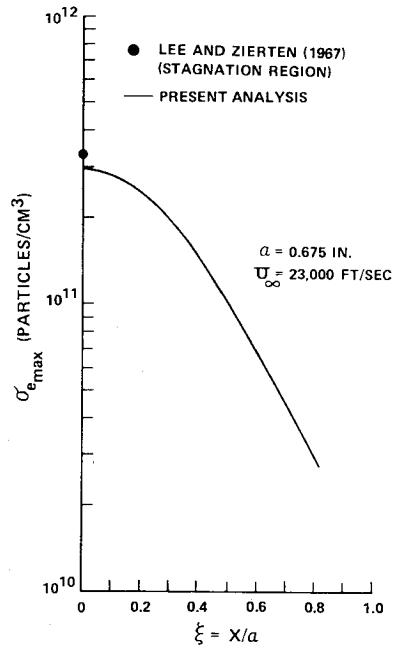

Fig. 8 Distributions of the maximum electron density along a blunt body, and its comparison with exact (numerical) solutions.

order of magnitude from the stagnation value. Thus, it is found that the prediction by the inviscid analysis is in greater error by as much as three orders of magnitude in the downstream region.

Another interesting result obtained in Ref. 7 was the applicability of the binary scaling principle to the merged-layer case in the stagnation region because of the negligible recombination in the flow. The results obtained from the present analysis also show this applicability in the stagnation region as well as in the downstream region.[11] Practically the same results were obtained when the present analysis was applied to the two cases involving different altitudes (ρ_∞) and nose radii (a) that varied by two orders of magnitude with the same values of $\rho_\infty a$ and the freestream velocity, thus supporting the applicability of the binary scaling principle to the ionized merged-layer flow cases.

IV. Concluding Remarks

The ionized nonequilibrium flow of a multicomponent air has been analyzed for the rarefied merged shock layer surrounding a blunt body. Solutions were obtained for a catalytic wall for various degrees of rarefaction in the downstream region as well as in the stagnation region by decoupling the species conservation equations from the other fluid dynamic equations and applying an integral method approach. The results indicate sizable influences of the wall cooling and species diffusion on the levels of the dissociation products in the viscous shock layer. It is found that increased rarefaction brings about reduction in these levels, especially on the electron-density levels, not only in the stagnation region but also in the downstream region of a blunt body. Comparison of the present results with another analysis is possible in the stagnation region, and reasonable agreement is obtained. Another result is that the binary scaling principle may be applied for the case of an ionized nonequilibrium flow in the merged layer of a blunt body due primarily to the dissociation-dominated nature of the chemical reaction at high altitudes. Finally, it is found that the inviscid analysis is found to overpredict the ionization level by as much as two orders of magnitude in the stagnation region, and three orders of magnitude in the downstream region, demonstrating significant viscous effects in the merged-layer flow cases on the electron-density levels.

Appendix A: Chemical Reaction Process

The six chemical reactions for air dissociation and ionization have been given in Eq. (11). The various reaction rates are tabulated in Table 1. The species production rates are

Oxygen (O):

$$w_O = m_O \cdot \rho^2 \cdot (S_1 + S_3 - S_4 - S_5) \tag{A1}$$

Nitrogen (N):

$$w_N = m_N \cdot \rho^2 \cdot (S_2 + S_3 + S_4 + S_5) \tag{A2}$$

Nitric Oxide (NO):

$$w_{NO} = m_{NO} \cdot \rho^2 \cdot (-S_3 - S_4 + S_5) \tag{A3}$$

NO^+ ion:

$$w_{NO^+} = m_{NO^+} \cdot \rho^2 \cdot S_6 \tag{A4}$$

where

$$S_1 = 2(k_{f1} n_{O_2} - \rho k_{b1} n_O^2) \cdot (n_N + 25 n_O + n_{NO} + 2n_{N_2} + 9n_{O_2})$$

$$S_2 = 2(k_{f2} n_{N_2} - \rho k_{b2} n_N^2) \cdot (n_{NO} + n_O + n_{O_2} + 2.15 \times 10^5/T \cdot n_N + 2.47 n_{N_2})$$

$$S_3 = (k_{f3} n_{NO} - \rho k_{b3} n_N n_O) \cdot [n_{N_2} + 20(n_N + n_O + n_{NO}) + n_{O_2}]$$

$$S_4 = k_{f4} n_O n_{NO} - k_{b4} n_N n_{O_2},\ S_5 = k_{f5} n_O n_{N_2} - k_{b5} n_N n_{NO}$$

$$S_6 = k_{f6} n_N n_O - k_{b6} n^2_{NO^+} \text{ and } n_i \equiv C_i/m_i$$

Appendix B: Species-Concentration Profiles

For the profiles of the chemical species concentration in the transformed coordinate system, third-degree polynomial forms are assumed. The boundary conditions used are a fully catalytic wall to all dissociation products, the species-conservation equation specialized to the solid body surface, and the modified Rankine-Hugoniot condition. They are, for i = O,N,NO and NO^+ (or e^-):

$$\begin{aligned} &\text{at } F = 0, \quad C_i = 0, \quad \left(\frac{\partial^2 C_i}{\partial F^2}\right)_b = 0 \\ &\text{at } F = 1, \quad C_{ie} + Q_{4i}\left(\frac{\partial C_i}{\partial F}\right)_e = 0 \end{aligned} \tag{B1}$$

where $Q_{4i} \equiv (K^2 G Sc_i \cdot dz/d\xi)^{-1}$ and the Schmidt number for O,N and NO is taken to be 0.75 and 0.375 for NO^+. Combination of Eq. (B.1) with the C_i-profiles yields

$$C_i(F) = E_i \cdot (F - N_{200} F^3), \ (i = \text{O,N,NO}) \tag{B2}$$

and

$$C_k(F) = E_k \cdot (F - N_{210} F^3), \ (k = NO^+, e^-) \tag{B3}$$

where $E_i \equiv (\partial C_i/\partial F)_b$, $N_{200} = (1 + Q_4)/(1 + 3Q_4)$, $N_{210} = (1 + 2Q_4)/(1 + 6Q_4)$, and $Q_4 \equiv 4/(3K^2 G dz/d\xi)$. Details of the formulation utilizing these profiles are discussed in Section II-D in the text.

References

[1] Hall, J. G., Eschenroeder, A. Q., and Marrone, P. V., "Blunt Nose Inviscid Airflows with Coupled Nonequilibrium Processes," *Journal of the Aerospace Sciences*, Vol. 29, No. 9, Sept. 1962, pp. 1033–1051.

[2] Ellington, D., "Approximate Method for Hypersonic Nonequilibrium Blunt Body Airflows," *AIAA Journal*, Vol. 1, No. 8, Aug. 1963, pp. 1901–1904.

[3] Blottner, F. G., "Prediction of the Electron Number Density Distribution in the Laminar Air Boundary Layer on Sharp and Blunt Bodies," AIAA Paper 68-733, Los Angeles, Calif., June 1968.

[4] Probstein, R. F. and Kemp, N., "Viscous Aerodynamic Characteristics in Hypersonic Rarefied Gas Flow," *Journal of the Aerospace Sciences*, Vol. 27, No. 3, March 1960, pp. 174–192.

[5] Chung, P. M., "Hypersonic Viscous Shock Layer of Nonequilibrium Dissociating Gas," Rept. TR R-109, 1961, NASA.

[6] Cheng, H. K., "The Blunt-Body Problem in Hypersonic Flow at Low Reynolds Number," Rept. AF-1285-A-10, 1963, Cornell Aeronautical Lab., Buffalo, N. Y.

[7] Lee, R. H. C. and Zierten, T. A., "Merged-Layer Ionization in the Stagnation Region of a Blunt Body," *Proceedings of the Heat Transfer and Fluid Mechanics Institute*, Stanford Univ. Press, Stanford, Calif., 1967, pp. 452–468.

[8] Dellinger, T. C., "Computation of Nonequilibrium Merged Stagnation Shock Layers by Successive Accelerated Replacement," AIAA Paper 69-655, San Francisco, Calif., June 1969.

[9] Hayes, W. D. and Probstein, R. F., *Hypersonic Flow Theory*, Academic Press, New York, 1959, pp. 375–395.

[10] Chung, P. M., Holt, J. F., and Liu, S. W., "Merged Stagnation Shock Layer of Nonequilibrium Dissociating Gas," *AIAA Journal*, Vol. 6, No. 12, Dec. 1968, pp. 2372–2379.

[11] Kang, S. W., "Hypersonic Low Reynolds-Number Flow over a Blunt Body with Mass Injection," *AIAA Journal*, Vol. 7, No. 8, Aug. 1969, pp. 1546–1552.

[12] Wray, K. L., "Chemical Kinetics of High Temperature Air," in *ARS Progress in Astronautics and Rocketry; Hypersonic Flow Research*, Vol. 7, edited by F. R. Riddell, Academic Press, New York, 1962, pp. 181–204.

[13] Vincenti, W. G. and Kruger, C. H., Jr., *Introduction to Physical Gas Dynamics*, Wiley, New York, 1965, pp. 230–231.

[14] Dunn, M. G. and Lordi, J. A., "Measurement of $NO^+ + e^-$ Dissociative Recombination in Expanding Air Flows," Rept. AI-2187-A-10, 1968, Cornell Aeronautical Lab., Buffalo, N. Y.
[15] Chung, P. M. and Anderson, A. D., "Dissociative Relaxation of Oxygen over an Adiabatic Flat Plate at Hypersonic Mach Numbers," Rept. TN D-140, 1959, NASA.
[16] Kang, S. W. and Dunn, M. G., "Integral Method for the Stagnation Region of a Hypersonic Viscous Shock Layer with Blowing," *AIAA Journal*, Vol. 6, No. 10, Oct. 1968, pp. 2031–2033.
[17] Kang, S. W., "Analysis of an Ionized Merged-Layer Hypersonic Flow over a Blunt Body," Rept. AI-2187-A-12, March 1969, Cornell Aeronautical Lab., Buffalo, N. Y.
[18] Chung, P. M. and Anderson, A. D., "Heat Transfer around Blunt Bodies with Nonequilibrium Boundary Layers," *Proceedings of the Heat Transfer and Fluid Mechanics Institute 1960*, Stanford University Press, Stanford, Calif., 1960, pp. 150–163.
[19] Kemp, N. H., Rose, P. H., and Detra, R. W., "Laminar Heat Transfer around Blunt Bodies in Dissociated Air," *Journal of the Aerospace Sciences*, Vol. 26, No. 7, July 1959, pp. 421–430.

JULY 1970 AIAA JOURNAL VOL. 8, NO. 7

An Experimental Investigation of the Compressible Turbulent Boundary Layer with a Favorable Pressure Gradient

DAVID L. BROTT,* WILLIAM J. YANTA,* ROBERT L. VOISINET†, AND ROLAND E. LEE‡
U. S. Naval Ordnance Laboratory, White Oak, Silver Spring, Md.

This paper describes the results of a detailed experimental investigation of a two-dimensional turbulent boundary layer in a favorable pressure gradient where the freestream Mach number varied from 3.8 to 4.6; the ratio of wall to adiabatic wall temperature remained constant at a value of 0.82. Detailed profile measurements were made with pressure and temperature probes; skin friction was measured directly with a shear balance. The velocity and temperature profile results are compared with zero pressure gradient and incompressible results. The skin-friction data are correlated with momentum-thickness Reynolds number and the pressure gradient parameter $\beta_\theta = (\theta/\tau_w)(dP/dx)$. The skin friction increases with decreasing β_θ for a constant value of momentum-thickness Reynolds number.

Nomenclature

A = constant in Eq. (4)
B = constant in Eq. (4)
C_f = skin-friction coefficient
H_u = incompressible shape factor
k = Karman's constant
M = Mach number
N = velocity profile exponent $u/u_e = (y/\delta)^{1/N}$
P = pressure
Re_θ = momentum-thickness Reynolds number
T = temperature
$\bar{T}$ = $(T_t - T_w)/(T_{te} - T_w)$
u = velocity
u_τ = shear velocity = $(\tau_w/\rho_w)^{1/2}$
u^+ = u/u_τ
x = distance along plate
y = distance normal to flow
y^+ = $u_\tau y/\nu_w$
β = Clauser's equilibrium parameter = $(\delta^*/\tau_w)(dP/dx)$
β_θ = pressure gradient parameter = $(\theta/\tau_w)(dP/dx)$
δ = boundary-layer thickness
ρ = density
δ^* = displacement thickness
θ = momentum thickness
τ = shear stress
ν = kinematic viscosity

Subscripts

aw = adiabatic wall
e = freestream conditions
o = supply conditions
w = wall conditions
t = total conditions

Presented as Paper 69-685 at the AIAA Fluid and Plasma Dynamics Conference, San Francisco, Calif., June 16–18, 1969; submitted June 11, 1969; revision received January 13, 1970. The investigation was sponsored by the Naval Air Systems Command under Task A32320/WR 009 02 03.

* Aerospace Engineer, Aerophysics Division, Aerodynamics Department. Associate AIAA.
† Aerospace Engineer, Aerophysics Division, Aerodynamics Department.
‡ Aerospace Engineer, Aerophysics Division, Aerodynamics Department. Member AIAA.

Introduction

THE work presented herein is part of an experimental program being carried out at the U. S. Naval Ordnance Laboratory (NOL) in which the turbulent boundary-layer flow is studied systematically and in detail with conventional pressure and temperature probes, and with a skin-friction balance. The earlier studies at zero pressure gradient and moderate heat-transfer rates were reported in Ref. 1. The present paper describes the results of the study of the turbulent boundary layer on the flat plate of the NOL Boundary-Layer Channel[2] along which the freestream Mach number varied from 3.8 to 4.6, and for moderate heat-transfer rates. Typical velocity and temperature profile data are presented along with skin-friction coefficients measured with a friction balance. The effect of the favorable pressure gradient on the boundary-layer flow structure and friction drag is discussed, and compared with supersonic zero pressure gradient and incompressible flow.

Nozzle Design

The main component of the NOL Boundary-Layer Channel is the two-dimensional supersonic half-nozzle shown in Fig. 1. One wall of the nozzle is a flat plate, 8 ft long and 12 in. wide. The opposite wall is a flexible plate which may be adjusted to give a prescribed Mach number distribution along the flat plate. Because of the numerous pressure gradient models